Chapter 3

Chitosan

Chapter 3

Chitosan

NORMA AUREA RANGEL-VÁZQUEZ[1]
FRANCISCO RODRÍGUEZ FÉLIX[2]
BÁRBARA-SUSANA GREGOR-VALDÉS[3]

[1]*División de Estudios de Posgrado e Investigación del Instituto Tecnológico de Aguascalientes, Ave. López Mateos # 1801 Ote. Fracc. Bona Gens CP. 20256 Aguascalientes, Aguascalientes, México*

[2]*Departamento de Investigación y Posgrado en Alimentos. Universidad de Sonora, Blvd. Luis Encinas y Rosales S/N Col. Centro, Hermosillo, Sonora, México*

[3]*Institute for Biotechnology and Bioengineering, Centre for Biological and Chemical Engineering, Instituto Superior Técnico, Av. Rovisco Pais 1, 1049-001 Lisboa, Portugal*

Abstract

Chitosan is a linear polysaccharide composed of randomly distributed β-(1-4)-linked D-glucosamine (deacetylated unit) and N-acetyl-D-glucosamine (acetylated unit). It is made by treating shrimp and other crustacean shells with the alkali sodium hydroxide. Chitosan has a number of commercial and possible biomedical uses. It can be used in agriculture as a seed treatment and biopesticide, helping plants to fight off fungal infections. In winemaking it can be used as a fining agent, also helping to prevent spoilage. In industry, it can be used in a self-healing polyurethane paint coating. In medicine, it may be useful in bandages to reduce bleeding and as an antibacterial agent; it can also be used to help deliver drugs through the skin.

Molecular modeling simulations are the most important tools to predict blend compatibility of polymers that are otherwise difficult to predict by experimental means. PM3 and AM1 *calculation is performed to obtain the Gibbs free energy, structural parameters, FTIR, molecular orbitals in chitosan.*

Keywords: Chitosan, Chitin, PM3, AM1, Simulation

3.1 Introduction

Among the novel families of biological macromolecules, whose relevance is becoming increasingly evident, are chitin and its main derivative, chitosan [1]. Potential and usual applications of chitin, chitosan and their derivatives are estimated to be more than 200. This wide range of applications includes biomedicine, food, biotechnology, agriculture and cosmetics, among others [1-2]. In addition to low cost, relative abundance, and biocompatibility, one of the appealing factors of using chitosan *in vivo* has been its wound healing properties [2].

Chitin and chitosan are described as a family of linear polysaccharides consisting of varying amounts of β (1→4) linked residues of N-acetyl-2 amino-2-deoxy-D-glucose (denoted in this review as A residues) and 2-amino-2-deoxy-Dglucose residues (denoted in this review as D residues). Chitin samples have a low amount of D units and hence the polymer is insoluble in acidic aqueous media (Figure 3.1).

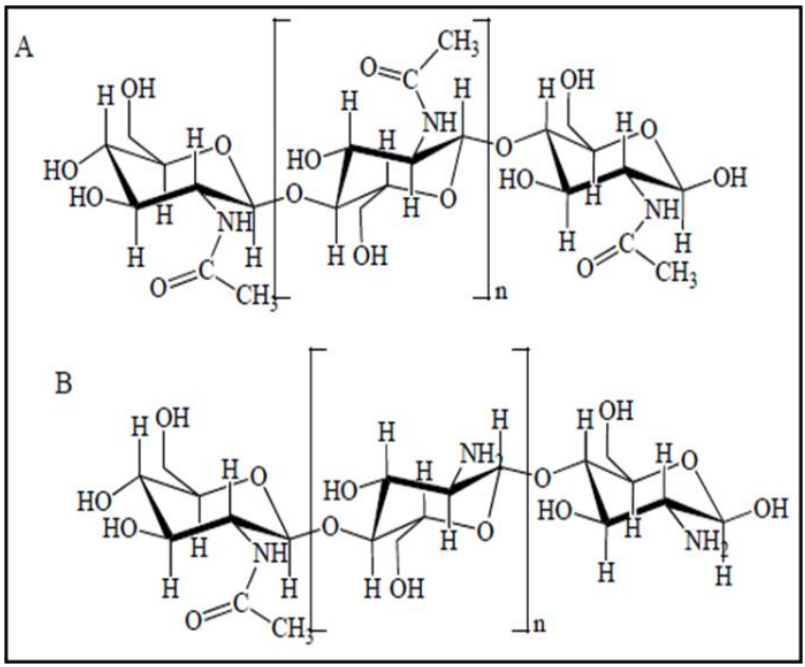

Figure 3.1 *Chemical structure of 100% acetylated chitin (a) and chitosan (b).*

On the other hand, the amount of D units in chitosan samples is high enough

to allow the polymer to dissolve in acidic aqueous media. Some authors consider that chitosan is the polymer with at least 60% of D residues. Chitin is the second most abundant natural polymer in nature after cellulose and it is found in the structure of a wide number of invertebrates (crustaceans' exoskeleton, insects' cuticles) and the cell walls of fungi, among others. On the other hand, chitosan only occurs naturally in some fungi (*Mucoraceae*) [1].

3.2 Synthesis

Chitosan is produced commercially by deacetylation of chitin, which is the structural element in the exoskeleton of crustaceans (such as crabs and shrimp) and cell walls of fungi. The degree of deacetylation (%DD) can be determined by NMR spectroscopy, and the %DD in commercial chitosans ranges from 60 to 100%. On average, the molecular weight of commercially produced chitosan is between 3800 and 20,000 Daltons. A common method for the synthesis of chitosan is the deacetylation of chitin using sodium hydroxide in excess as a reagent and water as a solvent. This reaction pathway, when allowed to go to completion (complete deacetylation) yields up to 98% product [3]. The amino group in chitosan has a pKa value of ~6.5, which leads to a protonation in acidic to neutral solution with a charge density dependent on pH and the %DA-value. This makes chitosan water soluble and a bioadhesive which readily binds to negatively charged surfaces such as mucosal membranes.

Chitosan enhances the transport of polar drugs across epithelial surfaces, and is biocompatible and biodegradable. Purified quantities of chitosans are available for biomedical applications. Chitosan and its derivatives, such as trimethylchitosan (where the amino group has been trimethylated), have been used in nonviral gene delivery. Trimethylchitosan, or quaternised chitosan, has been shown to transfect breast cancer cells, with increased degree of trimethylation increasing the cytotoxicity; at approximately 50% trimethylation, the derivative is the most efficient at gene delivery. Oligomeric derivatives (3-6 kDa) are relatively nontoxic and have good gene delivery properties [4].

3.3 Applications

The potential applications of modified chitosan in various important fields, such as environment, drug delivery, tissue engineering and other biomedical application are here discussed. An attempt is also made to discuss some of the current applications and future prospects of modified chitosan.

3.3.1 Drug Delivery

Chitosan has interesting biopharmaceutical characteristics such as pH sensitivity, biocompatibility and low toxicity. Moreover, chitosan is metabolised by certain human enzymes, especially lysozyme, and is biodegradable. Due to these favorable properties, the interest in chitosan and its derivatives in drug delivery applications have been increased in recent years. Moreover, in such applications it is also extremely important that chitosan be hydro-soluble and positively charged. These properties enable it to interact with negatively charged polymers, macromolecules and polyanions in an aqueous environment. Many works related with potential applications of chitosan and its derivatives can be found in literature. For instance, it has been shown that chitosan and its derivatives, such as *N*-trimethyl chitosan or *N*-carboxymethyl chitosan, have the special feature of adhering to mucosal surfaces, being useful for mucosal drug delivery.

Acrylic acid grafts of chitosan as possible means of creating hydrophilic and mucoadhesive polymers have been reported recently. Chitosan-grafted poly (acrylic acid) particles have been proposed as hydrophilic drug carriers for hydrophilic drugs and sensitive proteins. Kumbar et al. prepared microspheres of polyacrylamide-grafted-chitosan crosslinked with glutaraldehyde to encapsulate indomethacin (IM), a nonsteroidal anti-inflammatory drug used in the treatment of arthrhitis. Microspheres of grafted chitosan crosslinked with glutaraldehyde were prepared to encapsulate nifidifine (NFD), a calcium channel blocker and an antihypertensive drug.

N-Lauryl carboxymethyl chitosan with both hydrophobic and hydrophilic groups was studied in connection with the delivery of taxol to cancerous tissues. Other examples are related to the production of polymeric vesicles for encapsulation of hydrophobic compounds like bleomycin.

Some works related with intracellular delivery for gene therapy using modified chitosan-based materials were reported. In fact it has been argued that the most important application of alkylated chitosan is in DNA delivery such as proven with dodecyl chitosan. The high transfection efficiency of alkylated chitosan was attributed to the increasing entry into cells facilitated by hydrophobic interactions and easier unpacking of DNA from alkylated chitosan carriers, due to the weakening of electrostatic attractions between DNA and alkylated chitosan.

In another work, deoxycholic acid, which is the main component of bile acids,

was used to modify chitosan hydrophobically and to obtain self-assembling macromolecules for non-viral gene delivery system. The self-aggregate DNA complex from deoxycholic acid-modified chitosan was shown to enhance the transfection efficiency over monkey kidney cells. The feasibility of these chitosan self-aggregates for the transfection of genetic material in mammalian cells was investigated. Self-aggregates can form charge complexes when mixed with plasmid DNA. These self-aggregate DNA complexes are considered to be useful for transfer of genes into mammalian cells *in vitro* and served as good delivery system composed of biodegradable polymeric materials. PEGylation of chitosan in order to increase its solubility, elongate the plasma circulation time and prolong the gene transfer has been another proposed technique for the sustained DNA release. For example, Zhang et al prepared chitosan–DNA complexes conjugated with alpha methoxy-omega-succinimidyl PEG, and the gene expression was improved in comparison with the chitosan–DNA complex both *in vitro* and *in vivo*. Microspheres physically combining PEG-grafted chitosan (PEG-*g*-CHI) with poly (lactide-co-glycolide) (PLGA) were formulated by Yun et al. They reported that these microspheres were capable of sustained release of PEG-*g*-CHI/DNA for at least 9 weeks, and the rate of DNA release was not modulated by varying the amount of PEG-*g*-CHI.

In another work folate-PEG-grafted chitosan was synthesized and proposed for targeted plasmid DNA delivery to tumor cells. The authors found that folate conjugation in this system significantly improved gene transfection efficiency due to promoted uptake of folate receptor bearing tumor cells. *In vitro* and *in vivo* studies of gene transfection are being conducted in the laboratory to evaluate its gene transfection efficiency.

Very recently novel water-soluble nanoparticles that consist of a PAMAM dendrimer core with grafted carboxymethyl chitosan chains were successfully synthesized. The non-cytotoxicity and successful internalization of these dendrimer nanoparticles by two different types of cells, i.e., cell lines and primary cultures, was demonstrated in this work. The authors also showed that the dexamethasone-loaded nanoparticles induced the osteogenic differentiation of rat bone marrow stem cells *in vitro*. So, these novel dendrimer nanoparticles may be used as targeted drug-delivery carriers to cover a wide range of applications that involve the efficient intracellular delivery of biological agents to modulate the behaviour of cells.

Thiol-containing chitosan beads were synthesized in order to be used as a controlled and pH-responsive drug delivery system. It has been shown that P-chitosan beads have a great potential to be used as controlled drug release

systems through oral administration since the release in the highly acidic gastric fluid region of the stomach is avoided. Chitosan-based systems bearing β-cyclodextrin cavities have been proposed as a matrix for controlled release. Due to the presence of the hydrophobic β-cyclodextrin rings, these systems provide a slower release of the entrapped hydrophobic drug.

Finally, stimuli-responsive hydrogels have shown an improved drug loading capacity, and a sustained release behavior. In particular, systems that combine chitosan and PNIPAAm have shown drug release profiles that can be controlled by both pH and temperature, constituting very promising materials. This kind of smart systems has also been proposed for gene delivery. For instance, Sun et al. coupled a carboxyl-terminated NIPAAm/vinyl laurate (VL) copolymer with chitosan (PNVLCS) and examined the gene expression of PNVLCS/DNA complexes in C2C12 cells against temperature change.

The results indicated that the transfection efficiency of PNVLCS/DNA complexes was improved by dissociation of the gene from the carrier by temporarily reducing the culture temperature to 20 ℃. By contrast, naked DNA and lipofectamine did not demonstrate thermo-responsive gene transfection.

3.3.2 Tissue Engineering

The present generation of tissue engineering (TE) research is based on the seeding of cells onto porous biodegradable polymer matrixes. A primary factor is the availability of good biomaterials to serve as the temporary matrix. Recently, chitosan and its derivatives have been reported as attractive candidates for scaffolding materials because they degrade as the new tissues are formed, eventually without inflammatory reactions or toxic degradation. In TE applications the cationic nature of chitosan is primarily responsible for electrostatic interactions with anionic glycosaminoglycans, proteoglycans and other negatively charged molecules.

Some research works where the biological properties of chitosan and the mechanical properties of PLLA are combined have been reported. The *in vitro* fibroblast static cultivation on chitosan-grafted PLLA films for 11 days showed that the cell growth rate on these films was faster than in chitosan and decreased when the feed ratio of PLLA to chitosan increases. Surface functionalization of biodegradable PLLA was achieved by plasma coupling reaction of chitosan with PLLA.

The proliferation and morphology studies of two cell lines, L-929 (mouse fibroblasts) and L-02 (human hepatocytes), cultured on this surface showed that

cells hardly spread and tended to become round, but could proliferate at almost the same speed as cells cultured on glass surface. This insight will help to clarify the mechanism of the switch between cell growth and differentiation. This grafted polymer can be used to control themorphology and function of cells, and hence has potential applications in tissue engineering.

Very recently novel PLLA–chitosan hybrid scaffolds were proposed as tissue engineering scaffolds and simultaneously drug release carriers. In this innovative system a chitosan porous structure, in which cells and tissues would mostly interact, is created within the pore structure of a stiffer PLLA scaffold. It has been shown that thiolated chitosan can provide an adequate scaffold structure: due to the *in situ* gelling properties it seems possible to provide a certain shape of the scaffold material by pouring a liquid thiolated chitosan cell suspension in a mold.

Furthermore, liquid polymer cell suspensions may be applied by injection forming semi-solid scaffolds at the site of tissue damage. So they seem to be promising candidates for such applications. Surfaces that can induce the formation of an apatite layer *in vitro* demonstrate improved bone-binding properties and calcium phosphate growth on P-chitin fibers and P-chitosan films has been reported after soaking with Ca(OH)2.Water-soluble P-chitosans have been mixed with different calcium phosphate cements, showing an improvement in their properties, namely the mechanical strength, setting time, dissolubility of the start materials of the cements and they also bind calcium phosphate strongly afterwards. Moreover it has been shown that due to the smart nature of chitosan, the apatite formation of chitosan-grafted PLLA films reinforced with Bioglass® can be controlled by pH, which could also have relevance in bone TE applications [5].

Another approach regarding the chemical modification of chitosan for TE applications has been to introduce the specific recognition of cells by sugars. A recent example of the synthesis of sugar-bound chitosan can be found in the work of Kim et al.

They prepared mannosylated chitosan (MC) having the specific recognition to antigen presenting cells such as B-cells, dendritic cells and macrophages. In addition to applications in controlled drug release, PNIPAAmgrafted chitosan-based materials have been exploited for controlling cell adhesion/detachment by changing the incubation temperature above or below its LCST. Temperature responsive chitosan-graft-PNIPAAm was applied for the culture of mesenchymal stem cells (MSCs). Chitosan-*g*-PNIPAAm copolymers with

chondrogenic MSCs revealed the possibility of clinical applications, particularly as cell therapy technologies for treating vesicoureteral reflux [5].

3.4 Results and Discussion of Simulations Analyses

3.4.1 Optimization Energy

Table 3.1 shows the Gibbs free energy of the chitosan using different methods, in where the strong negative Gibbs free energy (ΔG) (see Table 3.1) calculated from the different methods shows that the electrostatic binding of chitosan is energetically favorable [6-7]. Attractive interactions between π systems are one of the principal non-covalent forces governing molecular recognition and play important roles in many chemical systems. Attractive interaction between π systems is the interaction between two or more molecules leading to self-organization by formation of a complex structure which has lower conformation equilibrium than of the separate components and shows different geometrical arrangement with high percentage of yield (Figure 3.2) [8]. It is evident from the reactional profiles that chitosan provides an abundance of reactive functional groups such as –COO−, $–NH_3^+$, –OH, $–CONH_2$, and $–NH_2$. The presence of such ionic functional groups may further provide a conductive surface environment for the growth and proliferation of the neural architecture on account of their mixed hydrophillicity/hydrophobicity and varied surface-to-charge ratio [9-10].

Table 3.1 *Gibbs energy free for chitosan structure.*

Method	ΔG (Kcal/mol)
AM1	-2273
PM3	-1966

3.4.2 Structural Parameters

Chitosan conformational diversity influences its solubility/physical state (soluble, gel, aggregate), porosity, particle size and shape (fiber, nanoparticle), ability to chelate metal ions and organic compounds, biodegradability and consequently its biological activity. The transition between these distinct conformational states is modulated by the percentage and distribution of acetyl groups. The level of chitosan acetylation and the distribution of N-acetyl groups along the chain have been shown to influence properties such as solubility, biodegradability and apparent pK_a values. Therefore, the percentage and

distribution of acetyl groups are key parameters for determining if chitosan can effectively interact with biological systems. The degree of acetylation can be experimentally determined by infra-red spectroscopy, ultra-violet spectroscopy and solid-state ^{13}C NMR. However, the interplay between chitosan acetylation and conformational transitions in solution cannot be characterized at high-resolution by experimental techniques. In these cases, the simulations are a more suitable approach [11]. The first task for a computational work was to determine the optimized geometry of chitosan. The molecular structure along with numbering of atoms of chitosan is as shown in Figure 3.2.

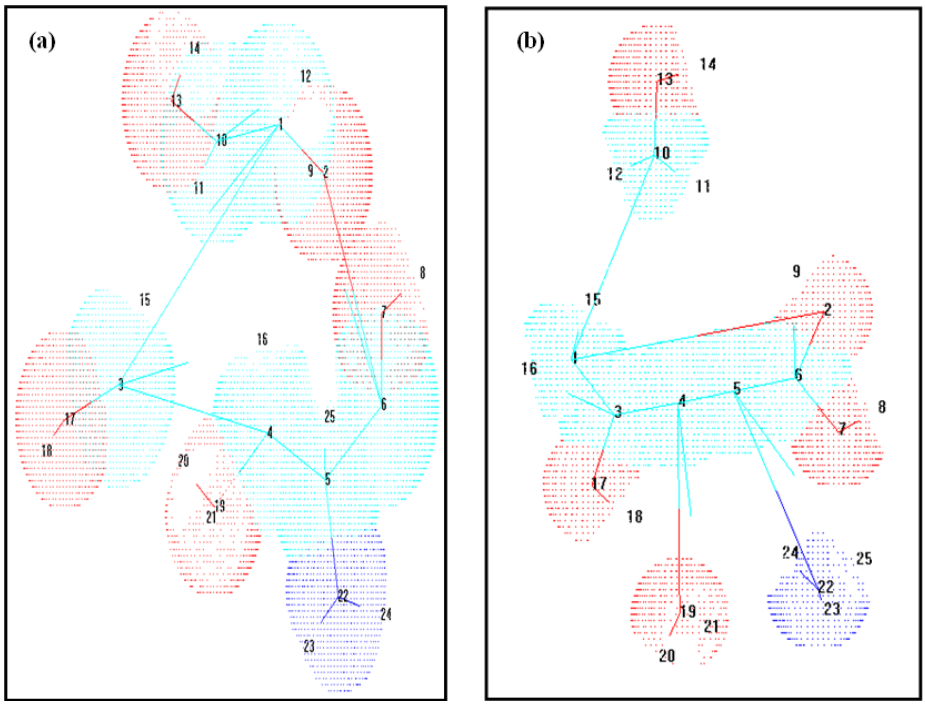

Figure 3.2 *Molecular geometry of chitosan, in where (a) PM3 and (b) AM1 method, respectively.*

The optimized structure parameter of chitosan calculated PM3 and AM1, is listed in Table 3.2 in accordance with the atom numbering scheme in Figure 3.2. From the structural data given in Table 3.2, it is observed that the various bond lengths are found to be almost same at PM3 and AM1 methods. According to results of bond length and bond angle, the deformations depend on the characteristic of the substituents [12].

Table 3.2 *Structural parameters calculated for chitosan employing PM3 and AM1 methods.*

Bond length (Å)	PM3	AM1
1-2	1.367	1.371
1-3	4.589	5.531
3-4	3.354	3.393
4-5	1.365	1.381
5-6	1.485	1.362
6-2	3.146	3.365
6-7	1.257	1.361
7-8	0.957	0.973
6-9	3.681	3.909
1-10	1.348	1.346
10-11	1.099	1.086
10-12	2.182	2.189
10-13	1.359	1.349
13-14	0.951	0.968
1-15	3.667	3.693
3-16	3.192	3.148
3-17	1.279	1.381
17-18	0.958	0.971
4-19	1.421	1.851
19-20	1.019	0.961
4-21	1.914	1.233
5-22	1.386	1.065
5-25	0.725	1.091
22-23	0.991	0.999
22-24	0.992	1.001

Bond angle (°)	PM3	AM1
1-2-6	115.268	123.573
2-6-5	98.399	96.940
6-5-4	119.376	116.572
5-4-3	150.21	148.461
4-3-1	50.956	53.858
3-1-2	100.271	103.634
2-6-7	26.025	29.504
2-6-7-8	129.148	130.086
2-6-9	13.263	18.710
2-1-10	123.171	125.225
1-10-11	126.737	121.535
10-13-14	109.542	108.531
3-17-18	108.82	108.754
4-19-20	105.369	106.559
5-22-23	116.588	113.319
5-22-24	115.174	123.844
5-6-7-8	179.005	171.428

3.4.3 FTIR Analyses

Vibrational spectral assignments have been performed on the recorded FTIR spectra based on the theoretically predicted wave numbers using PM3 and AM1, and have been collected in table 3.3. The infrared spectrum of chitosan (Table 3.3) is typically characterized by absorption regions as follows: at 3490 cm^{-1} which is attributed to the axial stretching of O–H and CH bonds; the CH stretching bond between 5776 and 3750 cm^{-1}, NH stretching at 3541 cm^{-1}, NH asymmetric stretching at 3452 cm^{-1} indicating presence of free amino group at

C_5 of glucosamine [13], at 3427 cm^{-1} is attributed to the combined peaks of the NH_2 and OH group stretching vibration [14], at 1216 cm^{-1} (–NH angular deformation) and 1567 cm^{-1} (–C–O–C– in glycosidic linkage), the intensity of some bands within the range 1500–1700 cm^{-1} that are related to amino and carbonyl moieties, evidenced that these groups interact mainly through electrostatic interactions and hydrogen bonding [15-16], between 3226 and 3028 cm^{-1} (aliphatic C–H band), and at 687, 287, and 257 cm^{-1} (C–O band) [17], the band in the range 3578 and 3407 cm^{-1} attributed to O–H stretching vibrations [18] and at 1635 cm^{-1} corresponding to the chitosan NH_2 [19-20].

Table 3.3 *The calculated frequencies using PM3 and AM1 methods, respectively.*

ASSIGNMENT	PM3 (FREQUENCIES CM^{-1})	AM1 (FREQUENCIES CM^{-1})
CH stretching	5776	--
CH stretching	3874	--
CH stretching	3750	--
NH symmetric stretching	3541	--
NH asymmetric stretching	3452	3452
CH stretching (CH_2 group)	3028	--
OH stretching	2836	--
C-CH_2-OH	1421	1418
C=O (amide I)	1650	1645
N-H (amide II)	1555	1558
C-N (amide III)	1380	1382
C-O	1050	1051
CH, NH, CO	687	--
C-C, C-N, C-O	287	257
OH	--	3578
OH and CH stretching	--	3491
OH stretching	--	3429
OH stretching	--	3407
CH stretching	--	3226
C-C	--	2190
C-O-H	--	1567
NH_2	--	1216
CH	--	925
CH and OH (CH_2-OH)	--	518

3.4.4 Electrostatic Potential

This finding suggests that hydrogen bond interactions, either intra-chains or between polymer chains and water molecules, play for a more important role in the solubility of chitin and chitosan than hydrophobic interactions. These results have further shown that fine tuning the electrostatic contributions in chitosan can be used to promote remodeling of its the physical state. Additional simulations have shown that the overall net charge and solubility of chitosan can be altered by changes in the pH. Comparison of the electrostatic response of a chitosan and chitin chains to pH changes shows a rather distinct surface charge profile for the two polymers [11].

Figure 3.3 shows the electrostatic potential of chitosan using PM3 and AM1, respectively. A portion of a molecule that has a negative electrostatic potential is susceptible to an electrophilic attack – the more negative the better. Molecular electrostatic potential (MESP), which is related to the electronegativity and the partial charge changes on the different atoms of the chitosan molecule, when plotted on the isodensity surface of the molecule MEPS mapping is very useful in the investigation of the molecular structure with its physiochemical property relationships.

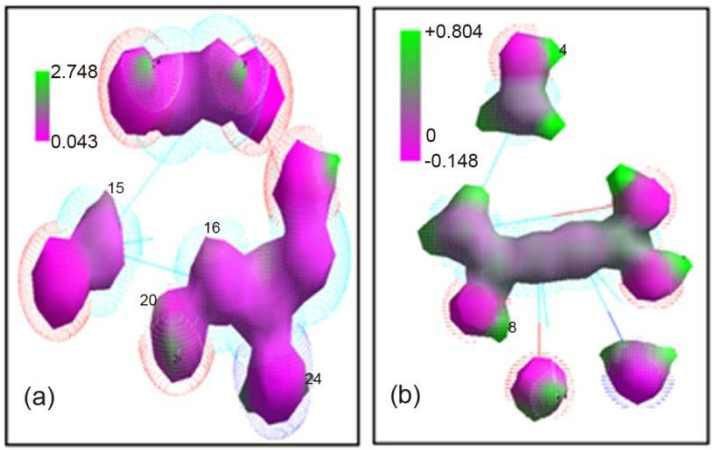

Figure 3.3 *Electrostatic potential of chitosan, in where (a) PM3 and (b) AM1, respectively.*

Pink and green areas in the MESP refer to the regions of negative and positive and correspond to the electron-rich and electron-poor regions, respectively, whereas the purple color signifies the neutral electrostatic potential [21]. The MESP in case of Figure 3.3(a) clearly suggest that each C-OH, C-H and NH bond represent the most negative potential region. Figure 3.3(b) shows

that C-C bond present neutral potential electrostatic region, C-O and NH bond represent the most negative potential region and finally the O-H represent the most negative potential region.

3.4.5 Molecular Orbitals

Hydrogen bonding, electrostatic interactions, van der Waals interactions (van der Waals bonds are mainly constructed with a balance of the exchange repulsion and dispersion attractive interactions), donor–acceptor interactions, hydrophilic–hydrophobic interactions, and π–π interactions are the main types of non-covalent interactions that are responsible for self-organization in biological systems. An evidence of charge transfer (CT) complexes had been reported in solid or in solution in a different field of chemistry. The basic electronic parameters related to the orbitals in a molecule are the HOMO and LUMO (energy and symmetry) of chitosan can give us idea about the ground and excited state proton transfer processes.

The HOMO and LUMO energy calculations (see Tables 3.4-3.5) reveal the existence of interactions and according to Mulliken's theory, formation of the (CT) complex involves transition of an electron from HOMO of donor to LUMO of acceptor [8]. Its highest occupied molecular orbital (HOMO) was provided primarily by nitrogen atom and its lowest unoccupied molecular orbital (LUMO) was provided mainly by the oxygen atom. Its reaction active sites were concentrated in -NH_2 and –OH [22]. Opposing π systems typically adopt parallelplaner (stacked or offset-stacked) geometry. The interaction between the donor and acceptor is characteristic of an electronic absorption band with low energy. One of these molecular complexes is π,π-complex between neutral molecules [8].

Table 3.4 *HOMO and LUMO orbitals for chitosan using PM3 method.*

ORBITAL	HOMO		LUMO	
	ENERGY (eV)	SYMMETRY (Å)	ENERGY (eV)	SYMMETRY (Å)
50	-16.60	32	-2.206	40
20	-23.25	14	1.293	55
10	-28.50	24	-1.097	45
5	-16.60	29	-2.206	40
-5	-2.215	39	-16.65	30
-10	-1.117	44	-28.19	25
-20	1.274	54	-23.71	15
-50	-2.210	39	-16.62	31

Table 3.5 *HOMO and LUMO orbitals for chitosan using AM1 method.*

ORBITAL	HOMO		LUMO	
	ENERGY (eV)	SYMMETRY (Å)	ENERGY (eV)	SYMMETRY (Å)
50	-12.57	31	2.492	42
20	-18.31	16	6.102	57
10	-14.22	26	4.502	47
5	-12.57	31	2.495	42
-5	2.489	41	-12.56	32
-10	4.058	46	-14.23	27
-20	6.092	56	-18.36	17
-50	2.489	41	-12.46	32

3.4.6 Conclusions

Empirical and semi-empirical mathematical models can be used to describe experimentally models are mechanistic theories. Molecular modeling is particularly useful to understand interactions between various kinds of molecules with different methods. The geometries energies of chitosan were computed by means of AM1 and PM3 methods. These calculations allowed us to retrieve the minimal energy conformation and investigate all possible conformations. The calculations confirmed that the most stable interactions involved the free amino site in a "pending complex". FTIR results are very similar between the different methods of analysis. The main absorption peaks of chitosan are observed at 1650-1645 cm^{-1}, attributed to C=O stretching (amide I), at 1558-1555 cm^{-1}, assigned to N-H bending (amide II), and at 1382-1380 cm^{-1}, assigned C-N stretching (amide III). The absorption peak at 1050 cm^{-1} is assigned to C-O stretching and the broad band above 3000 cm^{-1} corresponds to O-H and N-H bonds. Simultaneous structural parameters and IR of the different methods provide evidence for the charge transfer interaction between the donor and the acceptor groups. Vibrational analysis confirms that intramolecular charge transfer (ICT) must be responsible for the optical nonlinearity of the molecule. HOMO and LUMO energy gap explains the eventual charge transfer interactions taking place within the molecule. MESP plays an important role in determining stability of the molecule.

References

[1] Aranaz I, Meng bar M, Harris R, Pa ños I, Miralles B, Acosta N, Galed G and Heras A, Functional Characterization of Chitin and Chitosan, *Current Chemical Biology*, 3, 203-230, 2009.

[2] Park C J, Gabrielson N P, Pack D W, Jamison R D, Johnson A J W. The effect of chitosan on the migration of neutrophil-like HL60 cells, mediated by IL-8, *Biomaterials.* 30, 436–444, 2009.

[3] Zhuangdong Y. Study on the synthesis and catalyst oxidation properties of chitosan bound nickel (II) complexes. *Chemical Industry Times*. 21(5), 22–24, 2007.

[4] Kean T, Roth S, Thanou M. Trimethylated chitosans as non-viral gene delivery vectors: cytotoxicity and transfection efficiency. *J Control Release.* 103(3), 643–53, 2005.

[5] Alves N M, Mano J F, Chitosan derivatives obtained by chemical modifications for biomedical and environmental applications, *International Journal of Biological Macromolecules.* 43, 401–414, 2008.

[6] Mertins O, Dimova R. Binding of Chitosan to Phospholipid Vesicles Studied with Isothermal Titration Calorimetry, *Langmuir*. 27, 5506–5515, 2011.

[7] Hemalatha R, Chitra R, Rathinam J R, Sudha. P N, Synthesizing and characterization of chitosan graft co polymer: adsorption studies for Cu (II) and Cr (VI), *International Journal Of Environmental Sciences*. 2(2), 805-828, 2011.

[8] Shihab M S, AM1 semi-empirical calculation to study the nature of di- and tri-molecular assembly of π,π-aromatic interactions, *The Arabian Journal for Science and Engineering.* 35(2A), 95-113, 2010.

[9] Kumar P, Choonara Y E, Du Toit L C, Modi G, Naidoo D and Pillay V. Novel High-Viscosity Polyacrylamidated Chitosan for Neural Tissue Engineering: Fabrication of Anisotropic Neurodurable Scaffold via Molecular Disposition of Persulfate-Mediated Polymer Slicing and Complexation, *Int. J. Mol. Sci.* 13, 13966-13984, 2012.

[10] Zhu H Y, Fu Y Q, Jiang R, Yao J, Xiao L, Zeng G M, Novel magnetic chitosan/poly(vinyl alcohol) hydrogel beads: preparation, characterization and application for adsorption of dye from aqueous solution, *Bioresour Technol*. 105, 24-30, 2012.

[11] Cunha R A, Franca E F, Soares T A, Rusu V H, Pontes F J S and Lins R D. The Molecular Structure and Conformational Dynamics of Chitosan Polymers: An Integrated Perspective from Experiments and Computational Simulations, Biochemistry, Genetics and Molecular Biology. The Complex World of Polysaccharides. book edited by Desiree Nedra Karunaratne, ISBN 978-953-51-0819-1, Chapter 9.

[12] Kalninsh K K. Joint Experimental And Theorical study of the poly (styryl sodium) and poly (a-methylstyryl sodium) polymerization/ depolymerization. *Phys. Chem. Chem. Phys.* 3, 4542-4546, 2001.

[13] Jindal M, Kumar V, Rana V, Tiwary A K, Physico-chemical, mechanical and electrical performance of bael fruit gum–chitosan IPN films, *Food Hydrocolloids*, 30(1), 192-199, 2013.

[14] AbdElhady M M. Preparation and Characterization of Chitosan/Zinc Oxide Nanoparticles for Imparting Antimicrobial and UV Protection to Cotton Fabric, *International Journal of Carbohydrate Chemistry*, 1-6, 2012.

[15] Yuan Y, Wan Z L, Yin S W, Yang X Q, Qi J R, Liu G Q, Zhang Y, Characterization of complexes of soy protein and chitosan heated at low pH. *Food Science and Technology*, 50(2), 657-664, 2013.

[16] Pereira A E. Aldehyde-functionalized chitosan and cellulose:chitosan composites: application as drug carriers and vascular bypass grafts, Thesis for the Doctor of Philosophy degree in Pharmacy (Pharmaceutics), University of Iowa, 2011.

[17] Lertsutthiwong P, Noomun K, Khunthon S, Limpanart S. Influence of chitosan characteristics on the properties of biopolymeric chitosan–montmorillonite.

[18] George T S, Guru K S, Sankaranarayanan V N, Packiam K K. Extraction, Purification And Characterization Of Chitosan From Endophytic Fungi Isolated From Medicinal Plants. *World Journal of Science and Technology*, 1(4), 43-48, 2011.

[19] Islam M, Masum S, Rahman M, Molla A I, Shaikh A A, Roy S K. Preparation of Chitosan from Shrimp Shell and Investigation of Its Properties, *International Journal of Basic & Applied Sciences IJBAS-IJENS.* 11(01), 116-130, 2011.

[20] Britto D, Assis B G. Synthesis and mechanical properties of quaternary salts of chitosan-based films for food application. *International Journal of Biological Macromolecules*. 41(2), 198-203, 2007.

[21] Gayathri R, Arivazhagan M. Experimental (FTIR an FT-Raman) and theretical

(HF and DFT) investigation, NMR, NBO, electronic properties and frequency estimation analyses on 2,4,5.trichlorobenzene sulfonyl cl¿hloride. *Spectrochiica Acta Part A: Molecular and Biomolecular Spectroscopy*. 97, 311-325, 2012.

[22] Balanta D, Grande C D, Zuluaga F. Extracción, Identificación y Caracterización de Quitosano del Micelio de *Aspergillus Niger y* Sus Aplicaciones Como Material Bioadsorbente en el Tratamiento de Aguas, *Revista Iberoamericana de Pol ́meros*. 11(5), 297-316, 2010.